Energy 172 (2019) 566–579

Contents lists available at ScienceDirect

Energy

journal homepage: www.elsevier.com/locate/energy

Cofiring characteristics of coal blended with torrefied *Miscanthus* biochar optimized with three Taguchi indexes

Chao-Wei Huang [a], Yueh-Heng Li [b, *], Kai-Lin Xiao [b], Janusz Lasek [c]

[a] Department of Chemical and Materials Engineering, National Kaohsiung University of Science and Technology, Kaohsiung, 80778, Taiwan ROC
[b] Department of Aeronautics and Astronautics, National Cheng Kung University, Tainan, 70101, Taiwan ROC
[c] Institute for Chemical Processing of Coal, Ul. Zamkowa 1, 41-803, Zabrze, Poland

ARTICLE INFO

Article history:
Received 26 September 2018
Received in revised form
28 January 2019
Accepted 31 January 2019
Available online 1 February 2019

Keywords:
Torrefaction
Miscanthus biochar
Cofiring
Taguchi method
Thermogravimetric analysis

ABSTRACT

The main purpose of this study was the optimization of torrefaction conditions for biochar cofiring with new Taguchi indicators. However, the combustion characteristics of biochar cofiring in different furnaces and reactors are distinct. Examining optimal torrefaction conditions using the Taguchi method based on maximum energy or mass yields is paradoxical. Accordingly, three indicators, that is S index, proximate-based index (PA index), and elemental-based index (EB index), were proposed for solid fuel combustion. To study the combustion behavior of biochar torrefied under optimal conditions, a single pellet combustor was employed to record the characteristic time and gas emission at various reaction regions. Furthermore, the effects of ambient temperature and biomass blending ratio (BBR) on combustion behavior were investigated in the single pellet combustion experiment.

When the temperature was increased to 600 °C, the ignition delay time ranged from 8 to 29 s, whereas at 800 °C, the fuels were ignited within 4 s of each other. The total combustion times were shortened as the reaction rate increased. The total combustion time of Australian coal, raw Miscanthus, 50% blended biochar (S index), 50% blended biochar (PB index), and 50% blended biochar (EB index) were shortened by 19.3%, 18.9%, 14.2%, 12.9%, and 13.5%, respectively.

1. Introduction

Climate change threatens the survival of humans. However, the total elimination of fossil fuel use to mitigate extreme increases in CO_2 emissions is highly unlikely. According to the 2016 statistics of World Energy Resources, fossil fuels account for approximately 86% of global energy consumption to generate power and heat. Petroleum is the main fossil fuel and accounts for 32.94% of global primary energy consumption, with the contribution of coal and natural gas being more than 20% of global primary energy consumption. Therefore, the burning of fossil fuels is the main contributor to climate change due to enormous greenhouse gas (GHG) emissions. However, reducing fossil fuel use is inevitable. Numerous countries signed the Paris Agreement at the United Nations Climate Change Conference in 2015, with the aim to achieve GHG abatement. Consequently, many countries are developing alternative and renewable energy for fossil fuel substitution [1,2], such as nuclear power, solar energy [3,4], and hydraulic power, or advance clean fossil fuel combustion technology, such as oxyfuel combustion [5,6], oxy-enriched combustion [7], and flue gas recirculation combustion [8,9].

Currently, most countries burn coal to produce electricity and heat. Although coal-firing technology is low-cost and advanced, it releases enormous GHG and toxic emissions. Biomass cofiring with coal may achieve GHG abatement and reduce toxic emissions. Lasek and Kazalski [10] described that biomass cofiring can decrease CO_2 emissions because of the carbon neutrality of biomass, and meantime reduce toxic gas emission. Liu et al. [11] proposed that the synergetic effects of cofiring may reduce the emissions of pollutants such as NO_x. Fahlstedt et al. [12] found that coal cofiring with wood can reduce NO_x and SO_2 emissions. Andries et al. [13] cofired coal with straw in a 1.6-$MW_{thermal}$ pressurized fluidized bed combustion system. Due to the high volatile matter (VM) content of biomass, the temperature downstream of the freeboard was higher than the temperature of the coal-only case (i.e., approximately 30 K). Thus, CO, NO_x, and SO_2 concentrations were reduced in the freeboard. However, biomass cofiring can enhance combustion performance. Aerts et al. [14] cofired switchgrass with coal in a 50-

* Corresponding author.
E-mail address: yueheng@mail.ncku.edu.tw (Y.-H. Li).

https://doi.org/10.1016/j.energy.2019.01.168
0360-5442/

MW_e pulverized coal boiler. They found that the higher VM content of biomass can accelerate the burning of biochar. Armesto et al. [15] investigated the cofiring of low grade coal and pine chips in a circulating fluidized bed combustor and a bubble fluidized bed combustor. The results demonstrated the technical feasibility of fluidized bed as a clean technology for the combustion of low-grade coal/biomass blends.

Although biomass cofiring has advantages such as simple configuration and low cost, some operating difficulties (i.e., biomass storage and transportation, variability in biomass supply, fouling and corrosion, and furnace capacity reduction) remain when raw biomass is used, which must be solved [16]. Biomass has high moisture content, which results in reduced combustion efficiency [17]. The fuel properties of biomass are highly variable and heterogeneous. Even biomass obtained from different parts of the same plant can exhibit different compositions [18]. When raw biomass is stored for an extended period, it absorbs moisture, leading to the development of harmful fungi [19]. Biomass is also less brittle and more fibrous than coal, which leads to different grinding behaviors [20].

To overcome these problems, pretreatment methods have been proposed and utilized for improving the fuel characteristics of raw biomass, including hydrothermal carbonization, torrefaction, and slow pyrolysis [21–23]. Effective methods have been developed to densify the energy content of biomass and improve the hydrophobicity and grindability of biofuels. Torrefaction is a thermal degradation process conducted in an inert or limited-oxygen environment, in which biomass is slowly heated to temperatures ranging from 200 °C to 300 °C. Torrefied biomass has advantages such as reduced oxygen to carbon (O/C) and hydrogen to carbon (H/C) ratios, reduced transportation cost and time, enhanced energy density and gasification efficiency, and improved grindability and hydrophobicity. Wilk et al. [21] investigated the effect of three torrefaction temperatures and three residence times on the properties of torrefied wood biomass and sewage sludge. They concluded that torrefaction significantly improved the thermal properties of the wood biomass sample, and that the lignocellulose biomass material was suitable for torrefaction. Xue et al. [24] utilized torrefaction to improve the fuel characteristics of *Miscanthus giganteus*. They found that the torrefied *Miscanthus* had favorable properties compared with the raw material, such as low moisture and hemicellulose content, a lower O/C ratio, porous structures, larger specific surface area, and higher alkali metal content. All these features had a positive effect on *Miscanthus* gasification efficiency. Phanphanich and Mani [25] analyzed the fuel characteristics and grindability of pine chips torrefied at temperatures ranging from 225 °C to 300 °C. They highlighted that compared with untreated biomass, the specific energy consumption for grinding of torrefied biomass decreased up to 10 times for torrefied wood chips and up to six times for torrefied logging residues. Consequently, the torrefaction of biomass can improve fuel characteristics and enhance combustion efficiency.

Biomass can be fired directly or cofired with coal to reduce pollutant emissions. However, biomass cofiring has some risks and limitations. For example, many biomass materials contain a high fraction of alkali and chlorine in their ash. Thus, biomass cofiring may increase the fouling and corrosion rates of boiler heating surfaces [26]. In addition, the high moisture content in biomass causes a storage problem and reduces combustion efficiency. Sami et al. [27] proposed that the adiabatic flame temperature is decreased during cofiring. If the flame temperature is low, the fuel may barely be ignited, and the flame is unstable. Understanding solid fuel combustion is necessary for investigating biomass cofiring. In classical coal combustion, moist matter is evaporated in advance while coal is heated. When the solid temperature continues to increase, a pyrolysis reaction occurs, releasing pyrolytic gas products, which include noncondensable volatile gases (CH_4, CO, CO_2, and H_2) and other condensable organic compounds [28]. Once the ambient temperature is sufficiently high, oxygen from the ambient diffuses inward to the coal and reacts with outward volatile gases, resulting in the formation of a flamelet stabilized at a finite stand-off distance away from the coal. The volatile gases undergo oxidation within the gas film surrounding the particle. During this period, the surface of coal particle performs the devolatilization process, leading to the occurrence of volatile gas combustion. Accordingly, a homogeneous chemical reaction is initially dominant in coal combustion, until the volatile gases are gradually exhausted. After the volatile gases is exhausted, oxygen from the ambient diffuses inwardly to the surface of the coal particle and induces char combustion instead. At this moment, a heterogeneous chemical reaction is gradually predominant in coal combustion. Despite the fact of the heterogeneous combustion of fixed carbon (FC) and the combustion of volatile matter (VM) can proceed in parallel during volatile gas combustion, the dominance of chemical reaction is shifted.

Numerous methods can typically be used for optimization, such as trial-and-error, the one-factor-at-a-time experiment, the full factorial experiment, and the fractional factorial experiment. Among these optimization methods, the full factorial experiment is the most accurate because each parameter is considered. However, its operation is time consuming and expensive. The Taguchi method developed by Dr. Genichi Taguchi [29] has high accuracy and low cost. The advantages of this method are that numerous factors can be simultaneously optimized, and that much quantitative information can be extracted from a small-scale experiment [30]. It is versatile and has been used in various fields, such as medical, pharmaceutical, aerospace, and environmental engineering fields [31,32]. Regarding the application of the Taguchi method in biomass energy research, Chan et al. [33] constructed an L_9 orthogonal array to reduce the number of experimental runs; their experiments involved the catalytic pyrolysis of empty fruit bunches. In addition, they identified the optimal operating conditions for maximum bio-oil production by calculating the signal-to-noise (S/N) ratio. Li and Chen [34] employed the Taguchi method to optimize the torrefaction condition of empty fruit bunch, and the results presented the temperature and torrefaction pretreatment affects the chemical equilibrium in the gasification reaction. Chen et al. [35] optimized operating conditions for co-gasification by blending biochar with coal. They found that the influencing strength order of each factor was oxygen-to-fuel mass ratio (O/F ratio) > biomass torrefaction temperature > biomass blending ratio (BBR) > gasification pressure > inlet temperature > steam-to-fuel mass ratio (S/F ratio). Adu-Gyamfi et al. [36] used the Taguchi design of experimental methodology to determine the effects of different parameters on methane production from anaerobic digestion. They found that the type of immobilizing support has the maximum influence on methane productivity and contributes more than 60% of the overall impact, and they described an optimization approach that improved methane yield by more than 150%. From the literature, the Taguchi method appears to be a suitable method for identifying the influence of operating factors on the performance of gasification or pyrolysis, and it has been widely utilized for optimizing operation conditions. Optimizing torrefaction conditions for biochar is crucial. Biochar produced using optimal torrefaction conditions can facilitate and enhance the combustion performance of coal effectively [37]. According to their requirements, different solid fuel combustion systems have distinct optimal torrefaction conditions. For example, in a pulverized coal burner, the fuel must be ignited in a short time. Therefore, biochar with a short ignition time is suitable. By contrast, if the boiler

requires abundant thermal exothermicity, biochar with a high heating value is more effective. Consequently, discovering optimal torrefaction conditions based on the different requirements of solid fuel combustion systems is necessary. Therefore, in this study, the Taguchi method was used to discover optimal torrefaction conditions.

Biomass cofiring behavior has observed through thermogravimetric analysis (TGA) [38–40]. Although TGA is a convenient and efficient method for investigating the co-combustion behavior of fuels, it cannot represent an actual combustion situation because the fuel is heated at a fixed heating rate. Thus, to investigate the combustion behavior of fuels in actual combustion, the fuel experiment must be conducted in a pilot-scale burner. In addition, few studies have investigated the optimization of operating parameters for torrefaction and torrefied biomass cofiring [40]. Employing mass yield or energy yield as Taguchi indicator in the optimization may have distinct optimal result of torrefaction condition, leading to different flame behaviors. It appears to maximize energy or mass yield of torrefied biomass, but sacrifice the combustion efficiency and pollutant management. It implies that the appropriate selection of Taguchi indicator is pivotal to optimize the thermal pretreatment of biomass for biochar utilization in various combustion systems, such as pulverized coal furnaces and fluidized bed reactors. Accordingly, this study emphasizes to develop appropriate Taguchi indicators derived from combustion-relevant characteristics to optimize the torrefaction condition for biochar cofiring utilization. Ultimately, a single pellet combustion was employed to assess the chemical characteristic time and gas emission at various reaction regions for various biomass blending conditions.

2. Experimental methods

2.1. Thermogravimetric analysis

The weight loss of fuel ignited under dynamic conditions was estimated as a function of time or temperature by using a thermal analyzer (PerkinElmer, STA 8000). By determining the relation between weight and temperature through thermogravimetric analysis (TGA), some physical and chemical characteristics of fuel can be revealed at a certain temperature range. Moreover, based on the TGA curve, the differential thermogravimetric (DTG) curve can be generated, which presents the maximum weight loss peak.

In each experiment, approximately 15 mg of fuel with particle sizes <74 μm was placed in the crucible, and the heating rate was fixed at 20 °C/min within the range of 30–1000 °C. Nitrogen and air were delivered at a constant flow rate of 50 mL/min for pyrolysis and oxidation processes, respectively. The oxidation reaction provided the ignition temperature (T_i) and burnout temperature (T_b) [41,42], as shown in Fig. 1. The ignition temperature was defined as the minimum temperature at which fuel ignites spontaneously in an environment without an external source of ignition, and the temperature was obtained using the intersection method, for example at point B. The burnout temperature was defined as the temperature at which the fuel conversion reaches 99% [43]. The formula of fuel conversion is expressed as follows:

$$\alpha = \frac{W_i - W}{W_i - W_f} \times 100\%, \tag{1}$$

where W_i and W_f are the initial and final weights of fuel, respectively.

The results obtained were used to determine the combustion characteristic index (S index). This index is defined as follows [44]:

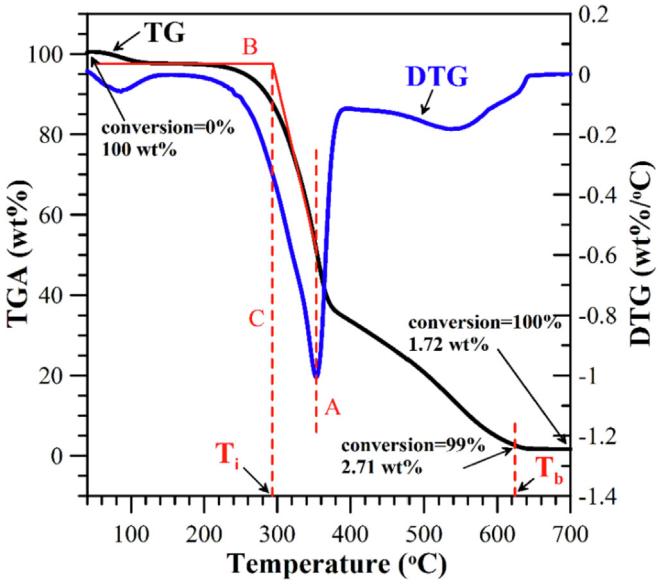

Fig. 1. Schematic of ignition temperature and burnout temperature.

$$S = \frac{\left(\frac{dW}{d\tau}\right)_{max} \times \left(\frac{dW}{d\tau}\right)_{mean}}{T_i^2 \times T_b}, \tag{2}$$

where W is the weight of fuel, τ is the time, and $(dW/d\tau)_{max}$ and $(dW/d\tau)_{mean}$ represent the maximum and average mass-loss rates, respectively.

This formula can be derived using the Arrhenius equation:

$$\frac{dW}{d\tau} = Ae^{-\frac{Ea}{RT}}, \tag{3}$$

where $dW/d\tau$ is the burning rate, ***A*** is the Arrhenius constant, ***Ea*** is the active energy, and ***T*** is the temperature of the fuel particle.

Deriving Eq. (3) with temperature can provide the following:

$$\frac{R}{E} \times \frac{d}{dT}\left(\frac{dW}{d\tau}\right) = \frac{dW}{d\tau} \times \frac{1}{T^2}. \tag{4}$$

When the temperature reaches ignition temperature, multiplying $\frac{(dW/d\tau)_{max} \times (dW/d\tau)_{mean}}{T_e}$ with Eq. (4) can provide the following:

$$\frac{R}{E} \times \frac{d}{dT}\left(\frac{dW}{d\tau}\right)_{T=T_i} \frac{(dW/d\tau)_{max}}{(dW/d\tau)_{T=T_i}} \times \frac{(dW/d\tau)_{mean}}{T_e} = \frac{\left(\frac{dW}{d\tau}\right)_{max} \times \left(\frac{dW}{d\tau}\right)_{mean}}{T_i^2 \times T_b}, \tag{5}$$

where $\left(\frac{dW}{d\tau}\right)_{max}$ is the maximum burning rate, $\left(\frac{dW}{d\tau}\right)_{mean}$ is the mean burning rate, and T_e is the end-burning temperature.

Each term of the formula represents a different physical parameter. Therefore, the formula obtained by combining these terms is called the combustion characteristic index (S index), which is shown in Eq. (2). A high S index implies that the fuel has higher combustion performance.

In addition to performing TGA, the TGA analyzer can perform proximate analysis. Proximate analysis provides the composition of the fuel in terms of gross components, such as moisture (M), volatile matter (VM), ash (ASH), and fixed carbon (FC). Fig. 2

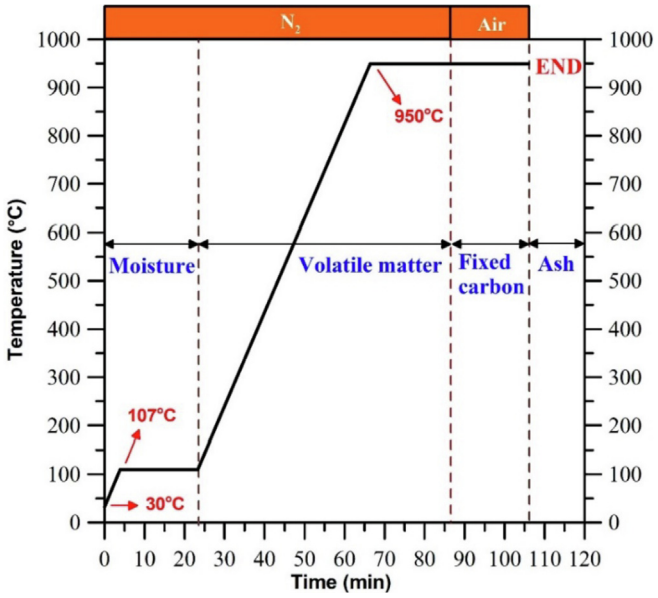

Fig. 2. Operating procedure of proximate analysis.

demonstrates the operating procedure of proximate analysis. First, the sample was heated to 107 °C in an inert atmosphere, and that temperature was maintained for 20 min, facilitating the removal of the moisture content of the fuel. Next, the sample was heated to 950 °C, and that temperature was maintained for 20 min. During this period, VM was released due to the pyrolysis reaction. The VM of a fuel is the condensable and noncondensable vapor released when the fuel is heated. Once the diluent gas shifted from nitrogen to air, a combustion reaction was induced. Eventually, the residue became ash. Ash is the inorganic solid reside after the fuel is completely burned. Its primary ingredients are silica, aluminum, iron, and calcium; small amounts of magnesium, titanium, sodium, and potassium may also be present. In general, the burning behavior of fuel is strongly related to its composition. Accordingly, performing proximate analysis of fuels is necessary.

2.2. Tubular furnace

Some properties of raw biomass render it unsuitable for cofiring; therefore, torrefaction was employed as a pretreatment method to ensure favorable chemical and physical properties of biomass. Torrefaction is a thermochemical decomposition process conducted in an inert or limited-oxygen environment, in which biomass is slowly heated. In this study, when the temperature reached 200°C–300 °C, hydrogen and carbon bonds were cleaved, and the hemicellulose structure extensively decomposed into volatiles, yielding a solid residue similar to charcoal-like biofuels. In general, torrefied biomass has some benefits, such as high energy density, favorable grindability and hydrophobicity, and high flowability and uniformity. In particular, a high pyrolysis temperature favors the yield of liquid and gaseous products, which reduces energy recovery in the biochar. Thus, the pyrolysis temperature is a pivotal parameter for solid fuel production from biomass, and a high pyrolysis temperature is crucial for maintaining the desired combustion properties [45].

Fig. 3 presents a schematic of the torrefaction system. The torrefaction system consisted of a tubular furnace, pressurized nitrogen tank, and condensation unit. During torrefaction, approximately 10 g of *Miscanthus* was crushed to a size smaller than 2.83 mm and was packed in a quartz cylindrical holder (2.5 cm

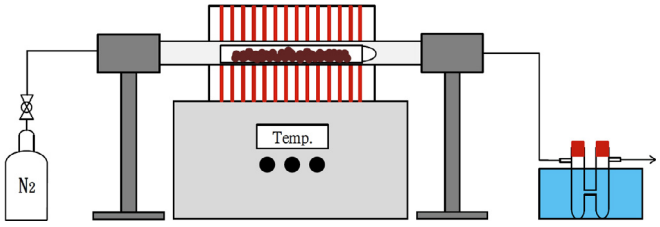

Fig. 3. Schematic of the torrefaction system.

in inner diameter and 22 cm in length). The holder was placed in the tubular furnace (3.4 cm in inner diameter and 50 cm in length). The effective heating length of the tubular furnace is 15.2 cm. Next, nitrogen was delivered at constant flow rates of 50, 100, and 150 cc/min to maintain the inert atmosphere inside the furnace. Torrefaction temperatures in the tubular furnace were 200 °C, 225 °C, 250 °C, 275 °C, 285 °C, and 300 °C, and the residence time maintained was 60, 90, and 120 min, respectively. After the completion of torrefaction, the quartz holder was removed from the tubular furnace and left to stand for 10 min until it reached room temperature. The samples were weighed before and after torrefaction to determine the mass yields. Finally, the torrefied biomass was analyzed to characterize its physical and chemical properties.

2.3. Single pellet combustion

In studies of solid fuel combustion, a single pellet furnace is often utilized to investigate the combustion behavior of fuel. The high heating rate in the furnace is similar to the actual combustion situation in an industrial-scale boiler. In addition, the single pellet furnace has the advantages of low cost, simple flow condition (laminar flow), and adjustable furnace temperatures. A simple flow condition is vital to decouple the flow effect from combustion. The adjustable furnace temperature mimics the variable temperatures within the chambers of various furnaces or reactors. It is convenient to investigate the combustion behavior of various pellet fuels in the different chamber temperatures of a drop-tube furnace. Fig. 4 presents a single pellet combustor and the corresponding measurement systems. The single pellet combustion system comprised two heating panels placed at a distance of 4.5 cm and the proportional-integral-derivative-controlled controller. The dimension of a heating panel is 30 cm in height, 10 cm in width and 20 cm in length. The heating panels were powered by 220 V/2 kW, and the chamber temperature of the single pellet furnace ranged from room temperature to 950 °C. Preheated air was continually delivered to the bottom of the single pellet furnace at a fixed flow rate of 3.5 L/min. The fuel pellet was made of fuel powder (approximately 0.8 g) and was compressed using a pelletizer with 2 tons of force held for 30 s. Thereafter, the pellet was dropped through the fuel conveying tube to the stainless mesh crucible with a diameter of 20 mm. The stand of mesh crucible is 32 cm in height. During the experimental process, the weight change of fuel was measured using an electronic balance in real time (~1 Hz). An observation window (30 cm in height and 4.5 cm in width) was placed in front of the single pellet furnace, and a 4 K video camera (SONY FDR-AX100) was used to record the combustion process with a frame rate of 30 fps and 1920 × 1080 spatial resolution. In addition, a gas analyzer (MRU, VarioPlus) was utilized to measure flue gas emissions, including O_2, CO, CO_2, and NO_x emissions. In this experiment, the fuel could be ignited if the chamber temperature was sufficiently high. Furthermore, the ignition delay, volatile burning time, and FC burning time of various fuels were obtained and compared. The ignition delay and volatile burning time of fuel were acquired

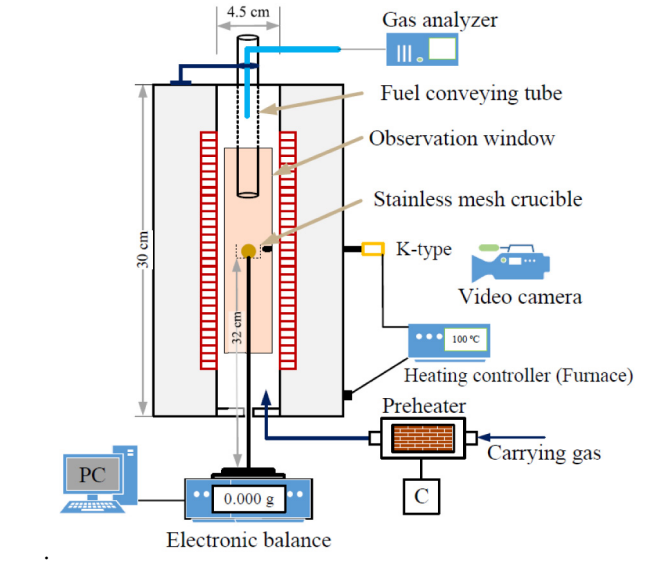

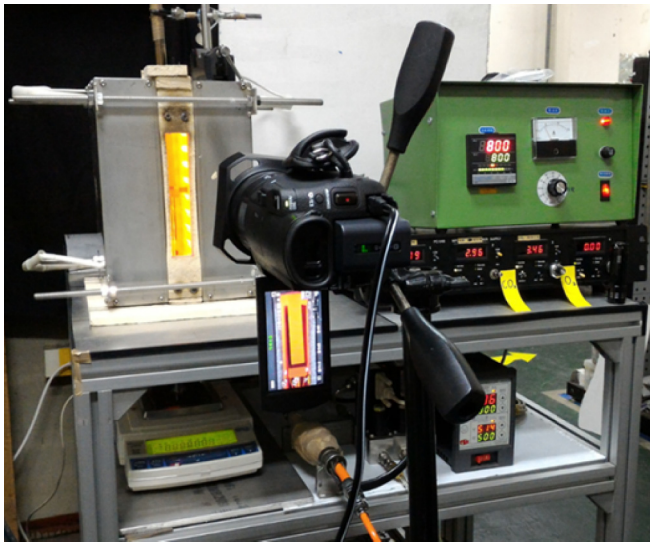

Fig. 4. Schematic and photograph of experimental apparatus.

and assessed through the photos taken by a 4 K video camera. Although this method was convenient, it may result in potential inaccuracies due to misjudgment of the images. Therefore, a more precise assessment of the chemical reaction time of single pellet combustion was developed, in which the chemical reaction time was estimated based on the weight change of fuel.

2.4. Taguchi method

2.4.1. Optimization of torrefaction conditions

To reveal the optimal conditions for torrefaction, the Taguchi method was used to conduct the minimal number of experiments, similar to a previous study [33]. The most crucial feature of the Taguchi method is the use of an orthogonal-array experimental design with a single analysis of variance. The S/N ratio was used to assess the quality characteristics deviating from the desired value. During the torrefaction of biomass, the characteristics of biochar were changed by setting the torrefaction parameters to different levels; the parameters were temperature, residence time, N_2 flow rate, biomass type, feed size, heating rate, and weight. They were assumed to be independent of each other. Among these parameters, temperature had the greatest influence on biochar. Thus, it was set at six levels in this study. To simplify the experiment, the residence time and N_2 flow rate were set to three levels, and the other parameters were fixed. Table 1 shows the orthogonal array L_{18} ($6^1 \times 3^6$), which effectively reduced the number of experimental runs from 54 to 18, saving on the experimental cost.

2.4.2. Selection of indicators

A literature review revealed that some researchers have investigated the combustion behavior of biofuels under different torrefaction conditions by using TGA [46,47]. Although the interaction between the surrounding temperature and the maximum weight loss of fuel can be obtained, the obtained interaction significantly differs from that in actual combustion due to the heating rate and operating temperature of the furnaces. Thus, in this study, the combustion behavior of solid fuels was investigated through single pellet combustion to reveal optimal torrefaction conditions for a specific biochar-cofiring combustion system. For this purpose, the appropriate indicators of the optimization of torrefaction conditions were proposed based combustion requirements. In the Taguchi method, an appropriate indicator is essential to achieve the optimization goal. For example, for a company that would like to maximize the remaining mass of biofuel, selecting the mass yield as an indicator for the optimization goal is appropriate. Therefore, three indicators were proposed based on three types of analyses, namely proximate analysis, elemental analysis, and TGA, as shown in Table 2. In proximate analysis, the contents of fuel can be analyzed in terms of M, VM, FC, and ash, whereas elemental analysis can detect the element content in fuels in terms of carbon, oxygen, nitrogen, and hydrogen. Regarding combustion, VM and FC are advantageous to solid fuel burning, and both parameters were placed in the numerator of the new indicator proposed in this study. By contrast, moisture and ash are unfavorable to solid fuel burning; thus, they were placed in the denominator of the new indicator. Therefore, the new indicator, named proximate-based index (PA index), was defined as the ratio of the product of VM and FC to the product of moisture and ash. Based on a Van Krevelen diagram [48], coal generally possesses lower H/C and O/C ratios than biomass. Thus, we considered that the combustion behavior of biofuels with low H/C and O/C ratios is more similar to that of fossil coal. Accordingly, another new indicator was proposed, which was the reciprocal of the product of H/C and O/C ratios, and this indicator was named elemental-based index (EB index). To explain the combustion characteristics of biomass-derived fuels, a comprehensive combustion indicator named S index was used. This indicator combined various physical properties associated with combustion behaviors, including fuel activity, fuel conversion, and fuel burning rate. In this study, PA index and EB index were proposed based on proximate and elemental analyses, respectively.

2.5. Operational procedure

In summary, the main purpose of this study is to investigate the combustion behavior of biochar under optimal torrefaction conditions. The study results can serve as a reference for future studies of biomass pretreatment under appropriate torrefaction conditions.

Fig. 5 shows the operational procedure of this experiment. First, 18 sets of the experiment were operated according to the L_{18} orthogonal array. To ensure consistent characteristics of the biomass material, raw *Miscanthus* was dried and crushed to a size smaller than 2.83 mm. Once the 18 sets of the experiment were completed, fuel characteristics were measured and the S/N ratio calculated. Through the calculation, optimal torrefaction conditions were obtained; thus, the biochar was produced under optimal

Table 1
Experimental layout using an L_{18} orthogonal array.

NO.	Temperature (°C)	Residence time (min)	Carrier gas flow rate (c.c./min)	Biomass material	Particle size (mm)	Heating rate (°C /min)	Weight (g)
1	200	60	50				
2	200	90	100				
3	200	120	150				
4	225	90	50				
5	225	120	100				
6	225	60	150				
7	250	90	50				
8	250	120	100				
9	250	60	150	Miscanthus	<2.83	10	5
10	275	60	50				
11	275	90	100				
12	275	120	150				
13	285	120	50				
14	285	60	100				
15	285	90	150				
16	300	120	50				
17	300	60	100				
18	300	90	150				

Table 2
Definition of three new indicators based on three types of analysis methods.

	Proximate analysis	Elemental analysis	Thermogravimetric analysis
Indicator	$\frac{VM \times FC}{M \times Ash}$	$\frac{1}{H/C \times O/C}$	S index

torrefaction conditions. Finally, the combustion behavior of the biochar was investigated through single pellet combustion.

3. Results and discussion

3.1. Fuel properties of Miscanthus and coal

Miscanthus is regarded as a C4 perennial energy crop. It can be divided into 15–20 species, such as *M. floridulus*, *M. nepalensis,* and *M. paniculatus*. *Miscanthus* is well known for its strong adaptability, rapid growth, low mineral content, favorable combustion properties, and high carbon fixation efficiency [49]. Thus, it is considered as a biomass feedstock with high developmental potential. *M. giganteus* has been studied in the European Union (EU) for its application in electricity generation, and currently, it is commercially used for electricity generation [50]. According to statistics, *Miscanthus* cofiring in coal power generating facilities can supply 12% of the EU's energy needs by 2050. However, few studies have discussed *Miscanthus* cofiring in Taiwan. Taiwan's climate is suitable for the growth of *Miscanthus*. Therefore, in this study, *M. floridulus* was used as a biomass feedstock and was cofired with coal. To ensure that a uniform source of biomass was utilized, *Miscanthus* was obtained from the Chiyai Agricultural Experiment Branch in Taiwan.

Regarding coal selection, Australian coal and Indonesian coal are the main fuel types used for power generation in Taiwan. Indonesian coal is cheaper than Australian coal, but Australian coal has the advantages of a high calorific value and low moisture content. To enhance heat release during biomass cofiring, Australian coal was chosen as the experimental feedstock. Table 3 presents the results of proximate and elemental analyses of raw *Miscanthus* and Australian coal conducted in a thermogravimetric analyzer, and the corresponding heat capacities for the two samples were detected using a calorimeter. The resulting atomic ratios of H/C and O/C for raw *Miscanthus* and Australian coal are also listed in Table 1. The characteristics of Australian coal and raw *Miscanthus* are notably different. Raw *Miscanthus* possesses 82.21% VM and 4.91% moisture but 5.85% FC. Australian coal has 46.32% FC, 33.49% VM, and only 1.31% moisture. The heating value of coal (6253 kcal/kg) is nearly twice that of raw *Miscanthus* (3831 kcal/kg). Element analysis revealed that Australian coal has high carbon, sulfur, and nitrogen content. *Miscanthus* has high carbon and oxygen content but low nitrogen content. In addition, biomass has no sulfur content. If the raw biomass is cofired with coal directly, this may lead to combustion problems. Consequently, raw *Miscanthus* must be pretreated before cofiring.

3.2. Measurement of Miscanthus biochar

To determine optimal torrefaction conditions based on the three aforementioned indicators, some fuel properties were measured in advance through proximate analysis, elemental analysis, and TGA. According to the L_{18} orthogonal array, the Taguchi method required 18 sets of the torrefaction experiment to be conducted. The optimal indicators were addressed, and they are listed in Table 2.

Biomass torrefaction aims to maximize energy and mass yields while reducing O/C and H/C ratios. Therefore, H/C and O/C ratios gradually reduced with an increase in the torrefaction temperature (Table 4). Torrefaction is primarily characterized by the degradation of hemicellulose. Dehydration and decarboxylation are the main reactions in this degradation and produce condensable and noncondensable products. In proximate analysis, moisture and VM content reduced with an increase in the torrefaction temperature, whereas the FC fraction significantly increased with increasing torrefaction temperatures. The value of the S index is based on the combustion characteristics of the fuel. According to Eq. (2), the S index is mainly determined by the ignition temperature. When the VM content of fuel is higher, it is prone to ignite at lower temperatures. Thus, the S index is proportional to the VM content. Table 4 demonstrates that the cases (No. 1, 2, and 3) of low torrefaction temperature retained high volatile content, resulting in a high S index. As the torrefaction temperature increased, hydrogen and oxygen atoms were released through dehydration and decarboxylation reactions, leading to the reduction of H/C and O/C ratios. Based on the Van Krevelen diagram [48], the fuel characteristics of the biochar with low H/C and O/C ratios were similar to those of coal. The biochar possessed higher heating value, but more ash residue was recorded. Nevertheless, according to the analysis of the effect of the residence time and carrier gas flow rate on biochar characteristics, fuel characteristics did not significantly change. This

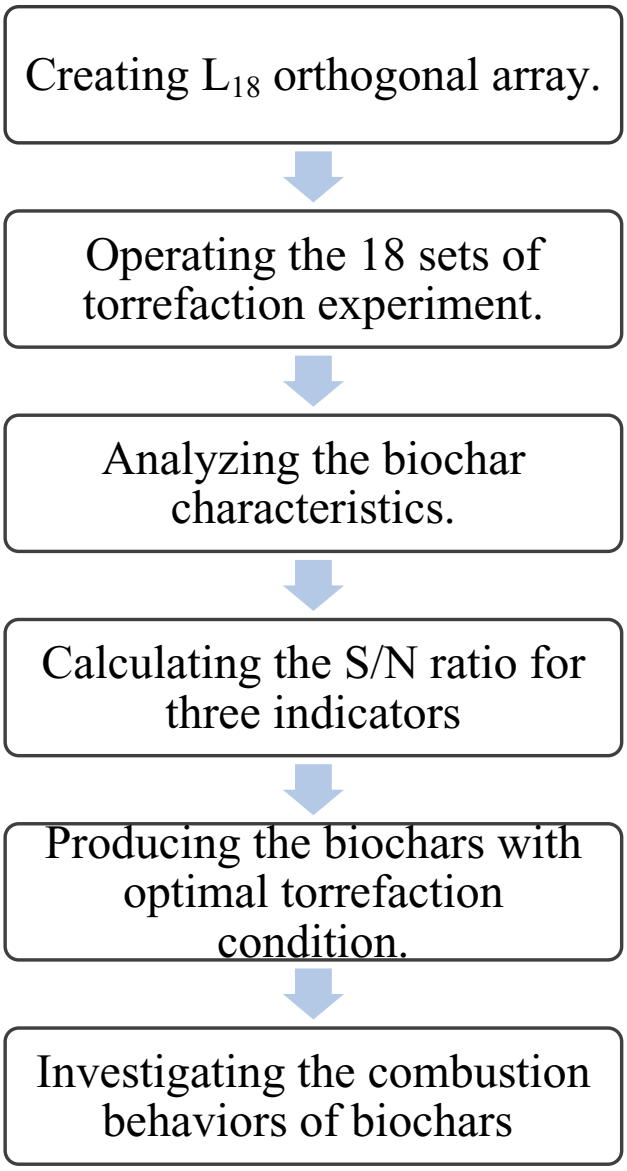

Fig. 5. Experimental flow diagram.

finding implies that the biochar characteristics are mainly influenced by the torrefaction temperature rather than the residence time and carrier gas flow rate.

Characteristically, the thermal decomposition of biomass occurs through a series of chemical reactions coupled with heat and mass transfer. Hemicellulose is the most active within a temperature range of 100 °C–260 °C, but its degradation is mainly initiated above 200 °C. Cellulose degradation occurs at an even higher temperature (>275 °C), but its degradation mainly occurs within a narrow temperature range of 270°C–350 °C. Lignin degradation gradually occurs over a temperature range of 250°C–500 °C, although its degradation is initiated within a temperature range of 80°C–90 °C. Fig. 6 shows photographs of raw *Miscanthus* and biochar at different torrefaction temperatures. The raw biomass had a coarser texture. The biomass underwent torrefaction at a temperature of 200 °C. The intrinsic moisture content of the biomass was released, and chemical decomposition was initiated; subsequently, the mass of the biomass was reduced from 10.2 to 8.67 g or by 15%. The mass yield was approximately 85%. In addition, the torrefied biomass became fragile and grindable, and the biomass was slightly

Table 3
Physical and chemical properties of raw *Miscanthus* and Australian coal.

Parameters	Raw *Miscanthus*	Australian coal
Proximate analysis (wt. %)		
Moisture (M)	4.91	1.31
Volatile matter (VM)	82.21	33.49
Fixed carbon (FC)	5.85	46.32
Ash	7.03	18.88
Elemental analysis (wt. %)		
C	38.30	73.30
H	5.85	4.17
O	55.27	5.25
N	0.58	1.14
S	0.00	0.52
Atomic ratio		
H/C	0.153	0.057
O/C	1.443	0.072
Calorific value (kcal/kg)		
High heating value (HHV)	3831	6253

red. When the torrefaction temperature was then increased to 275 °C, the biomass color changed to dark brown, and the mass significantly reduced from 10 to 6.4 g (approximately 36%) due to thermal degradation of its major hemicellulose content. The biomass was further heated to a high temperature of 300 °C and became much darker and more brittle. The mass decreased to 5.36 g compared with the original weight of 10.3 g, and the mass yield was 52%. In this stage, cellulose and lignin were chemically degraded. The energy density was anticipated to increase, but much of the energy was lost.

3.3. S/N ratio

Based on the analysis results for the 18 sets of experiments, the S/N ratios for each data set were determined. Taking case 1 as an example, Table 5 illustrates that the moisture content was 2.29%, VM 79.36%, FC 10.14%, and ash 8.21%. According to the proposed PA index, the PA index value of case 1 was 42.8. The formula of larger-the-better characteristics was used to calculate the S/N ratio based on Eq. (6):

$$\frac{S}{N} = -10 \times log\left[1 \Big/ (42.8)^2\right] = 32.63 \tag{6}$$

Table 5 shows the S/N ratio for the three indicators individually. To obtain the optimal torrefaction parameters, the mean of the S/N ratio at different levels was calculated. For example, the torrefaction temperature for cases 1–3 was fixed at 200 °C. Thus, the mean S/N ratio was as follows:

$$\frac{32.63 + 34.93 + 39.16}{3} = 35.57$$

The mean S/N ratio for each level could be calculated in a similar manner. The results are presented in Table 6. The maximum mean value was chosen as the optimal torrefaction parameter, as shown in Table 7. In addition, to understand the torrefaction parameters mainly influencing the fuel characteristics of biochar, the impact value was determined by subtracting the maximum and minimum values. A high value represented that the torrefaction parameter more significantly influenced the fuel characteristics of the biochar. Based on the calculation results, torrefaction parameters were ranked based on the degree of their influence: torrefaction temperature (high), residence time (intermediate), and N_2 flow rate (low). The result is consistent with that of a previous study [51].

Table 4
Characteristics analysis of *Miscanthus* biochar.

No.	Temperature (°C)	Residence time (min)	Carrier gas flow rate (c.c./min)	Proximate analysis (wt. %)				Elemental analysis (wt. %)		Thermogravimetric analysis (10^{-7})
				M	VM	FC	ASH	H/C	O/C	S index
1	200	60	50	2.29	79.36	10.14	8.21	1.56	0.91	58.2
2	200	90	100	1.67	80.45	9.65	8.33	1.56	0.96	60.0
3	200	120	150	1.66	77.17	14.00	7.17	1.58	0.94	59.1
4	225	90	50	1.51	81.00	9.32	8.17	1.48	0.85	55.6
5	225	120	100	1.47	76.06	14.96	7.51	1.61	0.87	55.0
6	225	60	150	1.03	77.53	13.10	8.34	1.49	0.84	56.4
7	250	90	50	0.96	74.47	16.40	8.17	1.36	0.81	53.5
8	250	120	100	1.38	75.65	14.47	8.50	1.34	0.80	48.9
9	250	60	150	1.31	74.54	16.36	7.79	1.33	0.86	32.7
10	275	60	50	0.83	65.98	22.30	10.89	1.10	0.83	21.5
11	275	90	100	0.68	68.66	20.11	10.55	1.24	0.80	18.9
12	275	120	150	0.95	60.91	26.73	11.41	1.16	0.75	17.1
13	285	120	50	1.22	61.61	24.15	13.02	1.07	0.67	11.1
14	285	60	100	0.83	59.25	27.09	12.83	1.11	0.72	17.4
15	285	90	150	1.24	55.22	29.83	13.71	1.13	0.76	15.2
16	300	120	50	1.25	58.87	29.02	10.86	0.94	0.66	17.8
17	300	60	100	0.98	57.64	29.51	11.87	1.05	0.63	14.1
18	300	90	150	0.78	54.88	31.88	12.46	1.00	0.65	22.0

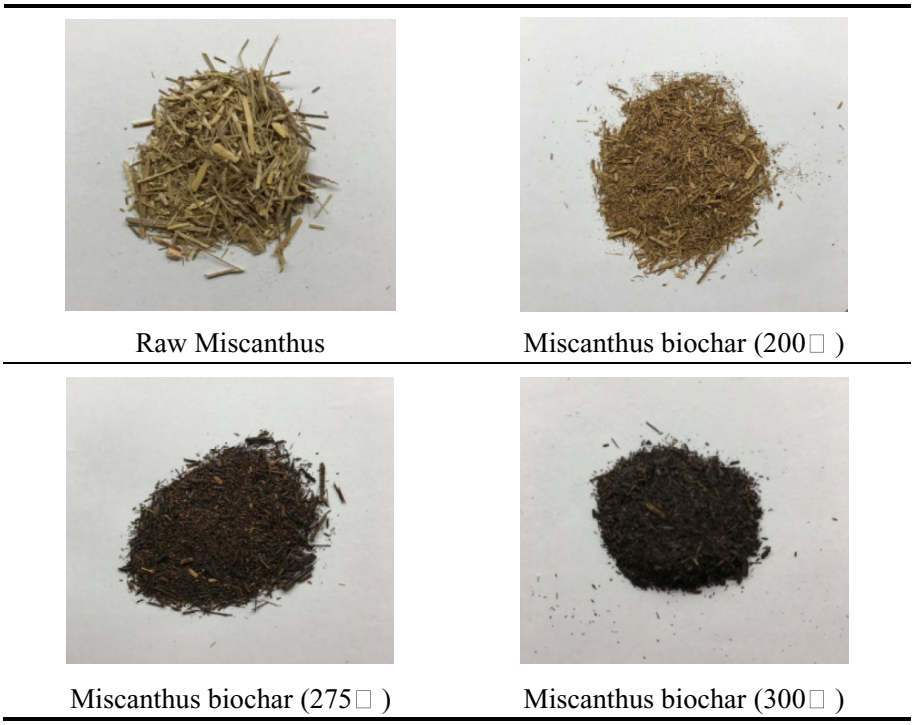

Fig. 6. Photographs of raw *Miscanthus* and torrefied biochar at different torrefaction temperatures.

3.4. Confirmation experiment

The final step of the Taguchi method was to validate the values and confirm the optimal conditions. The S/N ratio was predicted using the optimal levels of the parameters. The *PB* index was exemplified and was calculated as follows:

$$\frac{S}{N_{opt}} = \frac{S}{N_{AV}} + \left(A4 - \frac{S}{N_{AV}}\right) + \left(B1 - \frac{S}{N_{AV}}\right) + \left(C3 - \frac{S}{N_{AV}}\right) = 191.49,$$

where S/N_{AV} is the total mean of the S/N ratio, and S/N_{opt} is the mean of the S/N ratio at the optimal level. A4, B1, and C3 are maximal values of S/N response in three parameters, and the corresponding values are 49.17 for A4, 42.97 for B1, and 42.80 for C3 in Table 6.

From this calculation, the theoretical optimization value for the indicators could be obtained, as shown in Table 8. To validate the accuracy of the Taguchi method, the biochar underwent torrefaction under optimal conditions, and the resulting mean S/N values of the three indexes were determined. The error values for the three optimal indicators were less than 6% and were all acceptable. The PB index had a small error value of 1.22%, compared with the error value of 5.17% and 4.01% for the EB and S indexes, respectively. Consequently, the biochar torrefied under these three optimal conditions underwent single pellet to examine the combustion behavior and stability of the torrefied biochar cofiring.

Table 5
S/N ratios of the 18 experiments using three indexes.

No.	S/N (PB index)	S/N (EB index)	S/N (S index)
1	32.63	−3.00	−104.70
2	34.93	−3.52	−104.44
3	39.16	−3.43	−104.57
4	35.73	−2.00	−105.10
5	40.26	−2.91	−105.19
6	41.45	−2.00	−104.97
7	43.85	−0.90	−105.43
8	39.40	−0.59	−106.21
9	41.55	−1.20	−109.71
10	44.23	0.81	−113.35
11	45.69	0.05	−114.47
12	43.53	1.24	−115.34
13	39.43	2.88	−119.09
14	43.56	1.96	−115.19
15	39.73	1.38	−116.36
16	42.00	4.15	−114.99
17	43.30	3.57	−117.02
18	45.11	3.75	−113.15
Average	40.86	0.01	−110.52

Table 6
S/N response table for biochar (PB index).

	Temperature	Residence time	N2 flow rate
L_1	35.57	42.97	41.49
L_2	39.15	42.38	41.69
L_3	41.60	40.63	42.80
L_4	49.17	–	–
L_5	40.91	–	–
L_6	45.56	–	–
Max	49.17	42.97	42.80
Min	35.57	40.63	41.49
Max-Min	13.60	2.34	1.31
Mark	A	B	C
Rank	1	2	3

Table 7
Optimal torrefaction conditions based on three indexes.

Optimal torrefaction condition	PB index	EB index	S index
Temperature (°C)	275	300	200
Residence time (min)	60	120	90
N_2 flow rate (c.c./min)	150	50	100

Table 8
Validation of optimal torrefaction conditions.

	PB index	EB index	S index
Theoretical optimization value	191.49	1.74	64.8×10^{-7}
Experimental value	189.16	1.65	62.2×10^{-7}
Error value (%)	1.22	5.17	4.01

3.5. Single pellet combustion

In the combustion of pulverized coal, carbon char is produced after VM has been released from the coal particle and burned. The subsequent burnout of the carbon char is the limiting process that establishes the necessary residence time requirements. Coal combustion comprises two combustion processes: volatile combustion (homogeneous reaction) and char combustion (heterogeneous reaction). However, the composition of biochar is more diverse than that of coal; therefore, the combustion of biochar is anticipated to be distinct from that of coal. The contribution of VM combustion and char combustion is based on furnace selection, fuel substitution, and operational adjustment. In this study, single pellet combustion was employed to delineate the combustion behavior of coal and biochar pellets in a specific high temperature environment. The image of pellet reaction was recorded using the camera, and the resulting gas emission and weight loss with various time were simultaneously detected using the gas analyzer and the digital weight balance.

The fuel pellet was dropped into the crucible of the furnace, and the combustion process was recorded using a 4 K video camera with a frame rate of 30 fps and 1920 × 1080 spatial resolution. In general, single pellet combustion was characterized into four processes: moisture removal and devolatilization, volatile gas combustion, char combustion, and ash formation. Fig. 7 shows the timeline for the overall reaction process for single pellet combustion (50% coal−50% biochar), and labelled photography of single pellet combustion was snipped from the video and trimmed to the image with size of 20 mm × 70 mm. When a fuel pellet was dropped into the furnace, moisture and VM were released and underwent devolatilization. While volatile gases diffused into the surrounding atmosphere, combustible volatile gas mixed with oxygen and subsequently induced volatile gas combustion. The combustion process could be divided into two stages: volatile gas combustion and char combustion. In the volatile gas combustion stage, volatile gases, including H_2, CO, and CH_4, homogeneously reacted with oxygen. Defining the characteristic reaction time of volatile gas and char combustion based only on observation of the flame image is difficult. An overlapping region exists between these two stages, where volatile gas combustion was not completed, and char combustion had begun. However, some researchers have determined the burning time according to observation of the flame image [52]; that is, the visible flame disappearing denoted the onset of char combustion. Although this method can obtain an approximate characteristic time for volatile gas combustion, it is not accurate due to the mild and subtle flamelet adhering to the fuel pellet for a short time. This causes the misjudgment of the characteristic time. Therefore, developing an appropriate and mathematical approach to determine the characteristic time for those stages is necessary. In this study, the weight change of fuel pellet was recorded and employed to examine the characteristic time. In Fig. 8, the weight of the blended fuel (50% coal−50% biochar) decreased with time. Three turning points existed on these curves, splitting the combustion process into four stages. The region from the point A (time is zero) to point B showed a meager reduction on the weight curve. The region from points A to D pertained to moisture removal and devolatilization. According to the video, point B was the time of volatile gas ignition (8 s), namely the ignition point, whereas point D was the terminal time of devolatilization and volatile gas combustion (170 s). In the second region from points B to C, the slopes of the weight changing line became steeper. The fuel pellet was combusted through devolatilization, yielding immense volatile gas emissions. Subsequently, the obtained volatile gas burned and formed a flamelet that engulfed the fuel pellet, as shown the flame images at 15 s, 20 s and 30 s in Fig. 7. In this region, the surface reaction was dominated by pyrolysis and devolatilization, and the gas reaction was dominated by volatile gas combustion. In the third region from points C to D, the slopes of the weight changing line became smoother. This indicated that the devolatilization of the fuel pellet significantly reduced, corresponding to debilitated volatile gas combustion, as shown flame images at 50 s and 70 s in Fig. 7. Oxygen and carbon dioxide diffused inward of the fuel pellet and initiated char combustion. Therefore, point C represented the onset of char combustion, whereas point C represented the end of volatile gas combustion (70 s). This region denotes the coexistence of volatile gas combustion and char combustion. The dominant gas reaction was still volatile gas combustion, but this reaction gradually terminated. The

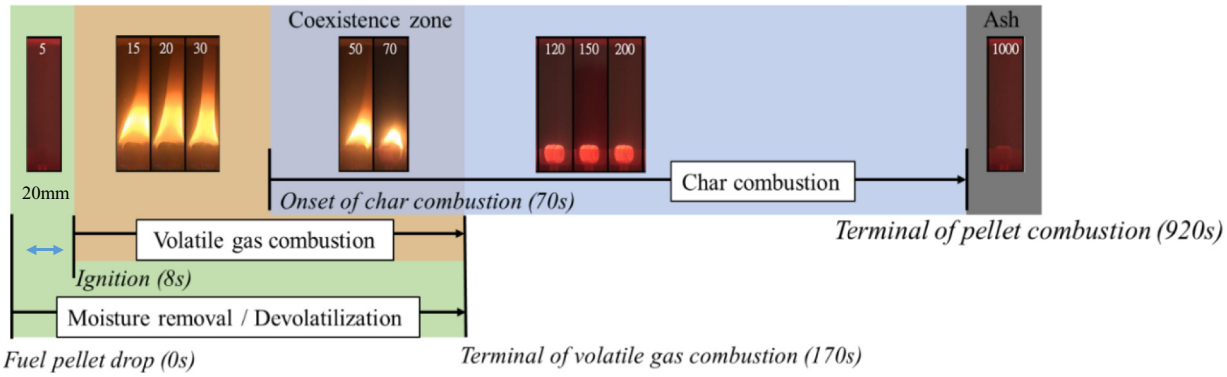

Fig. 7. Timeline for overall combustion process of a fuel pellet at a surrounding temperature of 600 °C.

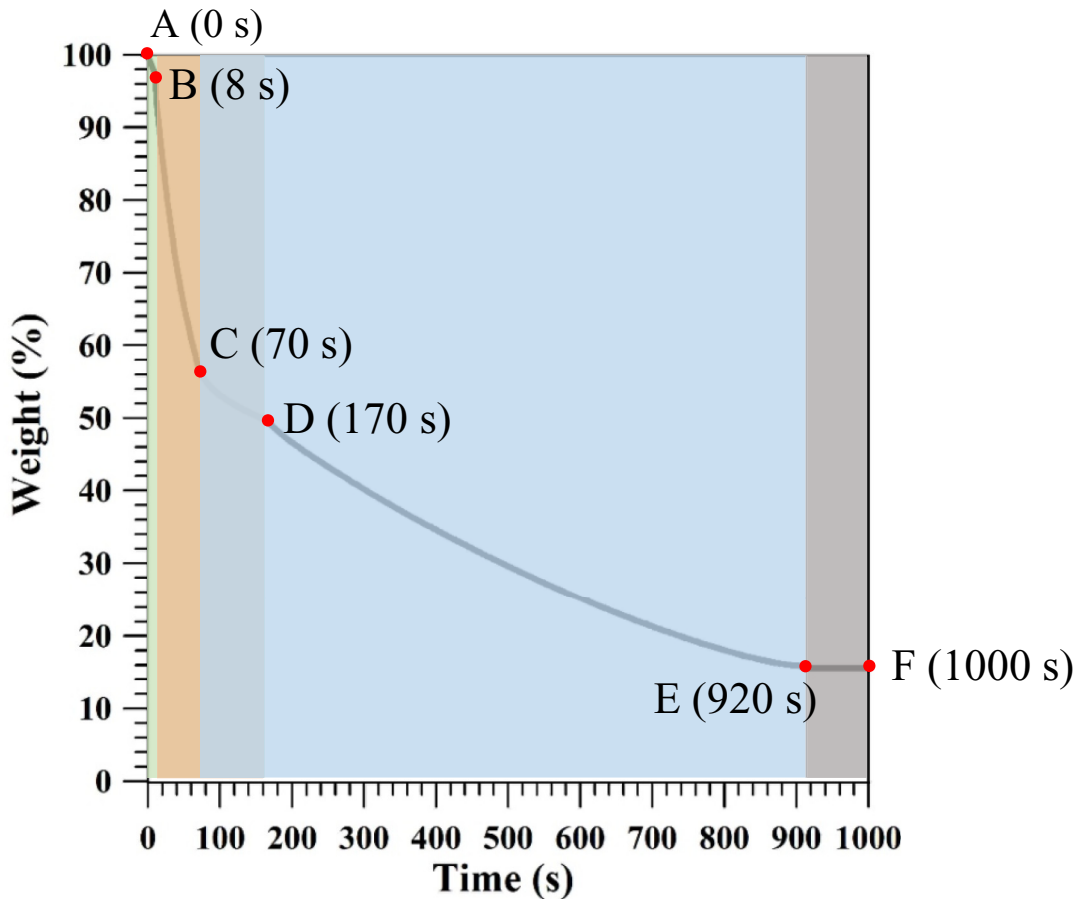

Fig. 8. Weight change of the fuel pellet against time for the blended fuel of 50% coal–50% biochar.

dominant surface reaction was a transition from devolatilization and volatile gas combustion to char combustion. In addition, the total time of gas volatile combustion is 162 s, which is equal to the subtraction between point D and point B. The fourth region from points D to E indicates the steady decline of fuel weight. Only long-lasting char combustion remained, and it lasted until no change in the fuel weight was present, that is, points E to F. Point E was the terminal time of char combustion. Consequently, the total time of char combustion is 850 s, which is equal to the subtraction between point E and point C. The char combustion has luminous surface on pellet instead of attached-on flamelets, as shown the images at 120 s, 150 s, and 200 s in Fig. 7. Through the definition of the weight change of the fuel pellet, the characteristic time of fuel ignition, volatile burning terminal, and char combustion terminal could be depicted.

Fig. 9 shows the measured emission gases during single pellet combustion. Flue gases were measured using the gas analyzer. O_2, CO, CO_2, and NO_x concentrations were detected, and CO and NO_x concentration were referred to the dry basis with a 3% O_2. NO_x formation originated from three sources: fuel NO_x, thermal NO_x, and prompt NO_x. Because *Miscanthus* contains less nitrogen, the contribution of fuel NO_x was low. Theoretically, when the environmental temperature exceeded 1600 °C, the nitrogen in the air participated in the chemical reaction and was converted to NO_x,

namely thermal NO_x. The NO_x concentration was too low and was neglected in the experiment.

Fig. 9a shows the reduction in oxygen and the increase in carbon monoxide after the fuel pellet was dropped into the furnace. This stage involved moisture removal, devolatilization, and mild pyrolysis. For the devolatilization process, some hydroxyl groups were removed and converted to CO and CO_2 emissions through pyrolysis. In addition, mild char combustion may have occurred through a heterogeneous combustion reaction with oxygen atoms ($C+½O_2 \rightarrow CO$), which caused significant changes in O_2 and CO concentrations. Followed by volatile gas combustion, combustible volatile gas was autonomously ignited and generated the flame. Meanwhile, the O_2 and CO were gradually consumed and simultaneously yielded large amounts of CO_2 because the produced volatile gas homogeneously reacted with the surrounding oxygen molecules to form CO_2. In this stage, volatile gas combustion was dominant, and the flame enveloped the fuel pellet, as shown in Fig. 7. After 70 s, volatile gas combustion ceased, and the gaseous flame was eventually extinguished. The fuel pellet was illuminated, and the fuel weight decreased monotonically. Char combustion was the monotonically chemical reaction in this stage. The O_2 diffused inward and reacted with the fuel surface to form CO_2, which then diffused outward. However, this reaction ($C + O_2 \rightarrow CO_2$) was not predominant in the carbon oxidation reaction because carbon monoxide was the preferred product at the combustion temperature. The CO_2 diffused inward, heterogeneously reacted with carbon, and produced CO through the reaction of $C + CO_2 \rightarrow 2CO$. CO homogeneously reacted with O_2 and produced CO_2. During this period, the heterogeneous reaction of carbon with CO_2 remained dominant compared with the heterogeneous reaction of carbon with O_2. Although the CO_2 concentration was rarely detected, the CO concentration was high during char combustion. Finally, after the solid combustion process was completed, the CO concentration sharply decreased, and the O_2 concentration decreased back to 21%.

3.6. Single pellet combustion at various furnace temperatures

In practical applications, different combustors have various operational temperatures. For example, the temperature of a circulating fluidized bed boiler is 400–500 °C, and the fuel pellets are conveyed into the furnace for combustion or gasification. However, in a pulverized coal boiler, the operational temperature is 900 °C because of the short residence time [53]. Therefore, sufficient heat should be provided to ignite the fuel in a short time. To investigate the effect of the furnace temperature on the combustion behavior of fuel, a single pellet combustion experiment at furnace temperatures of 600 °C and 800 °C was performed. Table 9 shows the time of the different reactions, including devolatilization, volatile gas combustion, and char combustion, for five fuel pellets. The devolatilization time also implied the ignition delay time of the fuel pellet. Five fuel pellets were selected for the single pellet combustion experiment, namely pure Australian coal, raw *Miscanthus*, 50% coal–50% biochar based on the PB index, 50% coal–50% biochar based on EB index, and 50% coal–50% biochar based on the S index. At the furnace temperature of 600 °C, Australian coal exhibited a long time for devolatilization or ignition delay and a short time for volatile gas combustion due to its inherently low VM content. However, the time for char combustion was long due to the high carbon content of fossil coal. Conversely, raw biomass possessed VM content. Raw *Miscanthus* exhibited a short time for devolatilization and ignition delay but a long time for volatile gas combustion. Compared with fossil coal, raw *Miscanthus* had a short time for char combustion and short total combustion time. Consequently, the combustion characteristic times for fossil coal and raw biomass were distinct. For the S index and PB cases, the blended fuel exhibited a long time for volatile gas combustion due to more VM. As the fuel pellets were dropped into the furnace, they underwent pyrolysis and initially released a large amount of volatile gases. Thus, the two fuel conditions were ignited at 11 and 8 s, respectively. The times of volatile gas combustion were 147 s for the PB case and 162 s for S index case. The times for volatile gas combustion were linked to those of raw *Miscanthus*. However, the fuels with high torrefaction degrees, for example blended fuel with the EB index, contained meager volatile gases; therefore, the time for devolatilization or ignition time extended to 12 s. The time for volatile gas combustion was 88 s, which was similar to that of fossil coal. Therefore, adjusting torrefaction conditions can achieve customization of the fuel properties of biochar to satisfy various furnace requirements.

To examine the effect of the furnace temperature on combustion, the furnace temperature was set to 800 °C for validation, as shown in Table 9 (b). At this furnace temperature, the fuels were ignited prior to 4 s. Higher surrounding temperature seemingly accelerated the devolatilization process and shortened the ignition

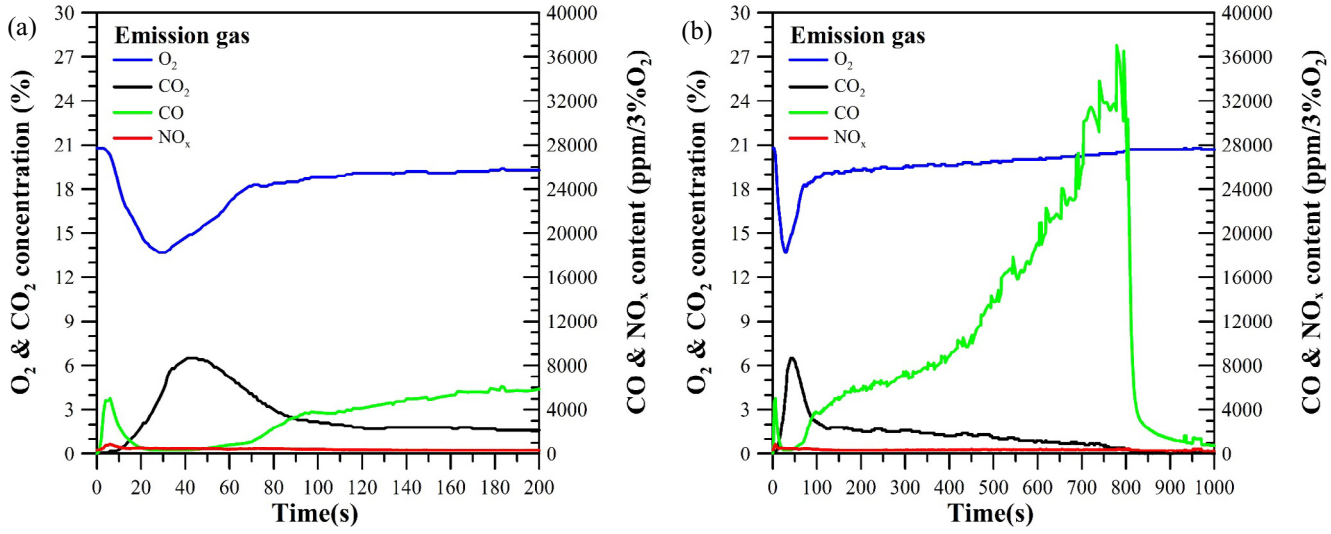

Fig. 9. Emission gases of the fuel pellet in single pellet combustion during (a) first 200 s and (b) 1000 s of reaction time.

Table 9
Combustion behavior of fuel in single pellet combustion (a) 600 °C (b) 800 °C.

(a) 600 °C furnace temperature				
Fuel	Moisture removal/Devolatilization	Volatile gas combustion	Char Combustion	Total
Australian coal	100	71	1634	1704
Raw *Miscanthus*	180	171	432	507
50% Blended fuel (PB index)	158	147	970	1025
50% Blended fuel (EB index)	100	88	998	1098
50% Blended fuel (S index)	170	162	850	920
(b) 800 °C furnace temperature				
Fuel	Moisture removal/Devolatilization	Volatile gas combustion	Char Combustion	Total
Australian coal	100	96	1315	1375
Raw *Miscanthus*	160	159	351	411
50% Blended fuel (PB index)	140	138	858	893
50% Blended fuel (EB index)	135	132	920	950
50% Blended fuel (S index)	150	148	739	789

delay time. In addition, the total reaction time of the five fuel pellets gradually decreased due to the high furnace temperature. The time for volatile gas combustion for the coal and coal-like condition, that is blended fuel (EB index), increased because more volatile gas was released through pyrolysis or gasification, leading to long volatile gas combustion. The high surrounding temperature increased the surface temperature of the fuel pellet, resulting in increased char combustion. This explained the reduction of the char combustion time. For raw biomass or biomass-like fuels, namely the blended fuels (PB index and S index), the tendency of the reaction characteristic time was similar to that of 600 °C. Regardless of the volatile gas combustion or char combustion process, the times reduced due to the chemical reactions of the fuel pellet.

The reaction times for the volatile gas combustion and char combustion were strongly related to the fuel's contents. In these two regions, the main influencing factors were air flow rate and diffusivity. The cases had the same operational conditions. Therefore, the reaction time was associated with the fuel content.

3.7. Single pellet combustion at various blending ratios

Although biomass cofiring can enhance the combustion performance of coal and reduce pollutant emissions, abundant or complete biomass substitution results in adverse effects. Research [51] has indicated that the heat released by blended fuel dramatically decreases depending on excessive biomass addition, and the overall combustion efficiency also deteriorates. To investigate the effect of BBR on combustion behavior, a single pellet combustion experiment with five BBRs (0%, 25%, 50%, 75%, and 100%) was systematically performed. Australia coal had a BBR of 0%, and the raw

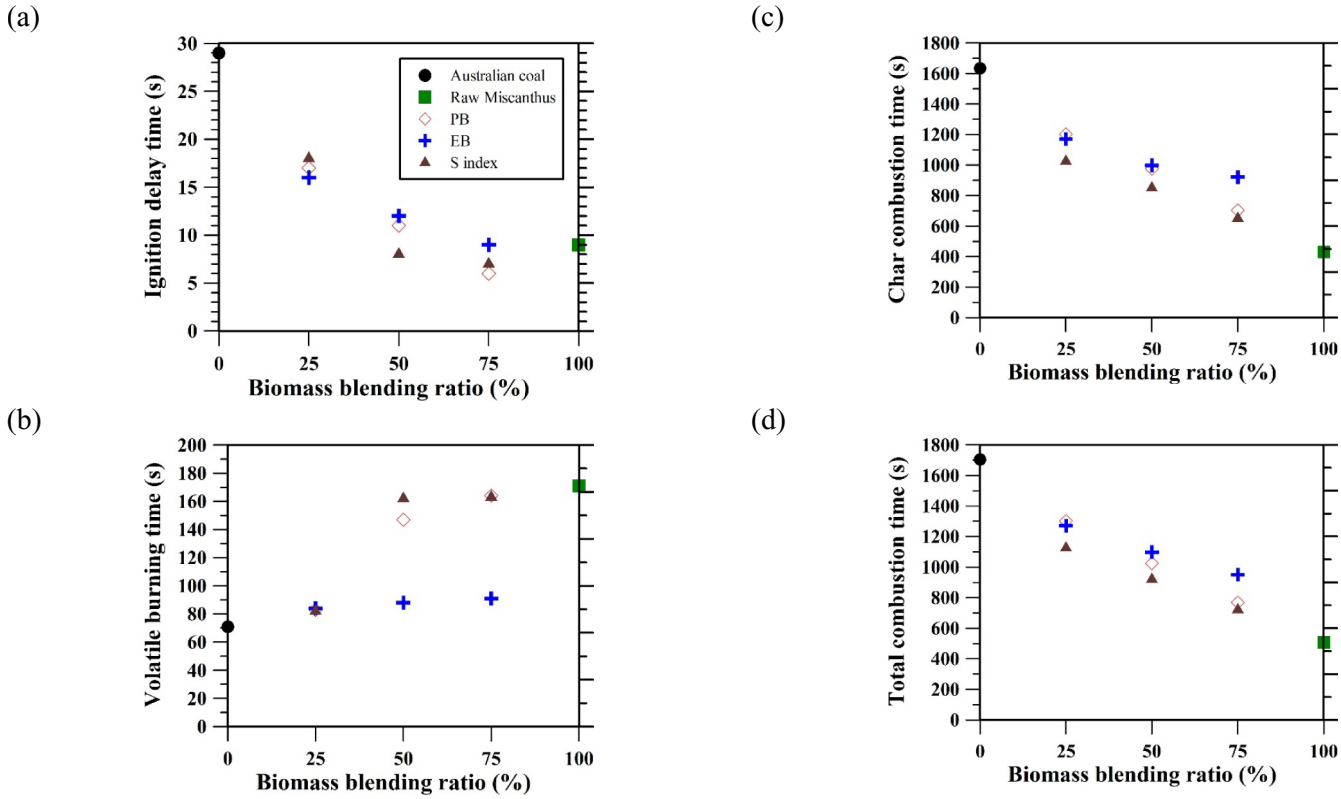

Fig. 10. Elapsed time at various stages for pellets with different BBRs at a furnace temperature of 600 °C. (a) Ignition time, (b) volatile gas combustion time, (c) char combustion time, and (d) total reaction time.

biomass had a BBR of 100%. Fig. 10 shows the elapsed time at different reaction stages, namely ignition delay time, volatile gas combustion time, char combustion time, and total reaction time for various BBR conditions. For the raw *Miscanthus*, because of the high VM content, the time for volatile gas combustion was longer than that of coal. By contrast, for Australian coal, a long time for char combustion was observed, which was due to its high FC content. The characteristics of the two fuels were different, which caused the elapsed time at different reaction stages to be distinct.

As biochar blended with coal, the time elapsed changed. Regarding ignition delay, the blended fuel was ignited earlier as the BBR increased. This phenomenon explained how biochar addition can improve the ignition delay for coal. In the region of volatile gas combustion, because of the low VM content in the condition of 25% BBR, the volatile gas combustion times were short for all cases. The combustion behavior of coal blended with 25% biochar was similar to that of pure coal. Until the BBR was more than 50%, the time for volatile gas combustion substantially increased for the blended fuel with the S index and PB index cases because these fuels possessed sufficient VM to extend the burning time. By contrast, the volatile burning time did not change significantly regardless of how much biochar with the EB index was added. This was because the biochar with the EB index had low volatile gas release, leading to a short volatile gas combustion time. Compared with the raw biomass, coal had a longer time of char combustion due to its high carbon content. With the increasing BBR, the time of char combustion reduced for the biochar with S and PB indexes. The decreasing tendency of char combustion time in the case of biochar with EB index was slower than those for the cases of biochar with S and PB indexes. Therefore, the biochar with optimal torrefaction conditions based on S and PB indexes retained the fuel properties of biomass; that is, high VM and low carbon content in fuel. This was called biomass-like biochar, which retained more combustion features of biomass. Conversely, the biochar torrefied under optimal conditions based on the EB index converted fuel to coal-like biochar; that is, it had low VM and high carbon content. However, char combustion accounted for the majority of the reaction time in the pellet combustion process; Figs. 10c and d illustrate a similar tendency. The char combustion time declined linearly with an increase in the BBR. When the BBR was high, the time difference among the different fuel components was apparent. Ultimately, the elapsed time for the different BBR conditions interpolated the elapsed time from the coal and raw biomass, with no synergetic effect.

4. Conclusions

The main purpose of this study was the optimization of torrefaction conditions for biochar cofiring. The Taguchi method is one of the most efficient and accurate optimization approaches. However, the combustion characteristics of biochar cofiring in different furnaces and reactors are distinct. The appropriate selection of Taguchi indicator is essential to optimize the thermal pretreatment of biomass from the point view of combustion. Accordingly, three Taguchi indicators were proposed for solid fuel combustion. To study the combustion behavior of biochar torrefied under optimal conditions, a single pellet combustor was employed to record the characteristic chemical reacting time and gas emission at various reaction regions. Furthermore, the effects of ambient temperature (600 °C and 800 °C) and BBR (0%, 25%, 50%, 75%, and 100%) on combustion behavior were investigated in the single pellet combustion experiment.

According to the result from the L_{18} orthogonal array, the fuel characteristics were significantly influenced by the torrefaction temperature. However, the residence time and N_2 flow rate had minor influence on the combustion characteristics of biomass. When the temperature was increased to 600 °C, the ignition delay time ranged from 8 to 29 s, whereas at 800 °C, the fuels were ignited within 4 s of each other. The total combustion times were shortened as the reaction rate increased. According to the calculation, the total combustion time of Australian coal, raw *Miscanthus*, 50% blended biochar (S index), 50% blended biochar (PB index), and 50% blended biochar (EB index) were shortened by 19.3%, 18.9%, 14.2%, 12.9%, and 13.5%, respectively. However, the ignition delay and char combustion times for biochar were linearly proportional to the BBR at the ambient temperature of 600 °C. For volatile gas combustion, regardless of the BBR, the reaction time of blended biochar (EB index) did not change significantly because it had low VM content, similar to coal. By contrast, for blended biochar (S index) and blended biochar (PB index), when the BBR was higher than 50%, the time for volatile gas combustion time was double that of the 25% blended fuel because the 50% blended biochar had more VM to burn.

Acknowledgments

Financial support for this work was provided by the Ministry of Science and Technology (Republic of China, Taiwan) under grant numbers MOST 106-2923-E-006-003-MY3, MOST 106-3113-E-006-002-CC2, and MOST 106-2218-E-992-304-MY2, and National Center for Research and Development (Poland) under grant number NCBR PL-TW IV/4/2017.

References

[1] Huang C-W, Liao C-H, Wu C-H, Wu JC. Photocatalytic water splitting to produce hydrogen using multi-junction solar cell with different deposited thin films. Sol Energy Mater Sol Cell 2012;107:322–8.
[2] Huang C-W, Liao C-H, Wu JC, Liu Y-C, Chang C-L, Wu C-H, et al. Hydrogen generation from photocatalytic water splitting over TiO2 thin film prepared by electron beam-induced deposition. Int J Hydrogen Energy 2010;35(21):12005–10.
[3] Li Y-H, Kao W-C. Performance analysis and economic assessment of solar thermal and heat pump combisystems for subtropical and tropical region. Sol Energy 2017;153:301–16.
[4] Li Y-H, Kao W-C. Taguchi optimization of solar thermal and heat pump combisystems under five distinct climatic conditions. Appl Therm Eng 2018;133:283–97.
[5] Yin C, Yan J. Oxy-fuel combustion of pulverized fuels: combustion fundamentals and modeling. Appl Energy 2016;162:742–62.
[6] Li Y-H, Chen G-B, Wu F-H, Hsieh H-F, Chao Y-C. Effects of carbon dioxide in oxy-fuel atmosphere on catalytic combustion in a small-scale channel. Energy 2016;94:766–74.
[7] Sanusi YS, Mokheimer EM, Shakeel MR, Abubakar Z, Habib MA. Oxy-combustion of hydrogen-enriched methane: experimental measurements and analysis. Energy Fuels 2017;31(2):2007–16.
[8] Li Y-H, Chen G-B, Lin Y-C, Chao Y-C. Effects of flue gas recirculation on the premixed oxy-methane flames in atmospheric condition. Energy 2015;89:845–57.
[9] Baltasar J, Carvalho MG, Coelho P, Costa M. Flue gas recirculation in a gas-fired laboratory furnace: measurements and modelling. Fuel 1997;76(10):919–29.
[10] Lasek JA, Kazalski K. Sulfur self-retention during cocombustion of fossil fuels with biomass. Energy Fuels 2014;28(4):2780–5.
[11] Liu H, Gibbs BM, Hampartsoumian. The significance of rank on coal reburning for the reduction of NO in drop tube furnace. In: 8th international symposium on transport phenomena in combustion; 1995.
[12] Fahlstedt I, Lindman E, Lindberg T, Anderson J. Co-firing of biomass and coal in a pressurized fluidised bed combined cycle. In: Proceedings of the 14th international conference on fluidized bed combustion in vancouver; 1997. p. 295–9.
[13] Andries J, Verloop M, Hein K. Co-combustion of coal and biomass in a pressurized bubbling fluidized bed. In: Proceedings of the 14th international conference on fluidized bed combustion in vancouver, vol. 1; 1997. p. 313–20.
[14] Aerts DJBK, Hoerning JM, Ragland KW. Co-firing switchgrass in a 50 MW pulverized coal boiler. In: Proceedings of the 59th annual American power conference; 1997. p. 1180–5.
[15] Armesto L, Cabanillas A, Bahillo A, Segovia JJ, Escalada R, Martinez JM, et al. Coal and biomass co-combustion on fluidized bed: comparison of circulating and bubbling fluidized bed technologies. In: Proceedings of the 14th international conference on fluidized bed combustion in vancouvervol. 1; 1997. p. 301–9.
[16] Jeguirim M, Dorge S, Loth A, Trouvé G. Devolatilization kinetics of Miscanthus

straw from thermogravimetric analysis. Int J Green Energy 2010:164–73.
[17] Orang N, Honghi T. Effect of feedstock moisture content on biomass boiler operation. Tappi J 2015;14:629–37.
[18] Iacovidou E, Hahladakis J, Deans I, Velis C, Purnell P. Technical properties of biomass and solid recovered fuel (SRF) co-fired with coal: impact on multi-dimensional resource recovery value. Waste Manag 2018;73:535–45.
[19] Kymäläinen M, Mäkelä M, Hildén K, Kukkonen J. Fungal colonisation and moisture uptake of torrefied wood, charcoal, and thermally treated pellets during storage. European journal of wood and wood products 2015;73(6):709–17.
[20] Gil M, García R, Pevida C, Rubiera F. Grindability and combustion behavior of coal and torrefied biomass blends. Bioresour Technol 2015;191:205–12.
[21] Wilk M, Magdziarz A. Hydrothermal carbonization, torrefaction and slow pyrolysis of Miscanthus giganteus. Energy 2017;140:1292–304.
[22] Chen G-B, Li Y-H, Lan C-H, Lin H-T, Chao Y-C. Micro-explosion and burning characteristics of a single droplet of pyrolytic oil from castor seeds. Appl Therm Eng 2017;114:1053–63.
[23] Yang SI, Wu MS, Wu CY. Application of biomass fast pyrolysis part I: pyrolysis characteristics and products. Energy 2014;66:162–71.
[24] Xue G, Kwapinska M, Kwapinski W, Czajka KM, Kennedy J. Impact of torrefaction on properties of Miscanthus giganteus relevant to gasification. Fuel 2014;121:189–97.
[25] Phanphanich M, Mani S. Impact of torrefaction on the grindability and fuel characteristics of forest biomass. Bioresour Technol 2011;102(2):1246–53.
[26] Kalisz S, Ciukaj S, Tymoszuk M, Kubiczek H. Fouling and its mitigation in PC boilers Co-firing forestry and agricultural biomass. Heat Tran Eng 2015;36(7–8):763–70.
[27] Sami M, Annamalai K, Wooldridge M. Co-firing of coal and biomass fuel blends. Prog Energy Combust Sci 2001;27:171–214.
[28] Piriou B, Vaitilingom G, Veyssière B, Cuq B, Rouau X. Potential direct use of solid biomass in internal combustion engines. Prog Energy Combust Sci 2013;39(1):169–88.
[29] Taguchi G. Introduction to quality engineering: designing quality into products and processes. 1986.
[30] Ross PJ. Taguchi techniques for quality engineering. Mcgraw-hill book company; 1988.
[31] Ghani JA, Choudhury IA, Hassan HH. Application of Taguchi method in the optimization of end milling parameters. J Mater Process Technol 2004;145:84–92.
[32] Yang WH, Tarng YS. Design optimization of cutting parameters for turning operations based on the Taguchi method. J Mater Process Technol 1998;84(1):122–9.
[33] Chen G-L, Chen G-B, Li Y-H, Wu W-T. A study of thermal pyrolysis for castor meal using the Taguchi method. Energy 2014;71:62–70.
[34] Li Y-H, Chen H-H. Analysis of syngas production rate in empty fruit bunch steam gasification with varying control factors. Int J Hydrogen Energy 2018;43(2):667–75.
[35] Chen WH, Chen CJ, Hung CI. Taguchi approach for co-gasification optimization of torrefied biomass and coal. Bioresour Technol 2013;144:615–22.
[36] Adu-Gyamfi N, RaoRavella S, Hobbs P J. Optimizing anaerobic digestion by selection of the immobilizing surface for enhanced methane production. Bioresour Technol 2012;120:248–55.
[37] Kopczyński M, Lasek JA, Iluk A, Zuwała J. The co-combustion of hard coal with raw and torrefied biomasses (willow (Salix viminalis), olive oil residue and waste wood from furniture manufacturing). Energy 2017;140:1316–25.
[38] Annamalai K, Thien B, Sweetenb J. Co-firing of coal and cattle feedlot biomass (FB) fuels. Part II. Performance results from 30 kWt (100,000) BTU/h laboratory scale boiler burner. Fuel 2003;82(10):1183–93.
[39] Lu R, Purushothama S, Yang X, Hyatt J, Pan WP, TRiley J, et al. TG/FTIR/MS study of organic compounds evolved during the co-firing of coal and refuse-derived fuels. Fuel Process Technol 1999;59(1):35–50.
[40] Li Y-H, Lin H-T, Xiao K-L, Lasek J. Combustion behavior of coal pellets blended with Miscanthus biochar. Energy 2018;163:180–90.
[41] Zeng HC, Yao B, Qii JR. Studies of combustion and slagging characteristics of anthracite blends with bituminous coal. Ranshao Kexue Yu Jishu 1996;2:181–9.
[42] Qiu SH, Wang ZY. Analysis of combustion properties of mixed coal. Shandong Jiancai Xueyuan Xuebao 1997;11:27–31.
[43] Lua JJ, Chen WH. Investigation on the ignition and burnout temperatures of bamboo and sugarcane bagasse by thermogravimetric analysis. Appl Energy 2015;160:49–57.
[44] Ren X, Meng J, Moorea AM, Chang J, Goub J, Park S. Thermogravimetric investigation on the degradation properties and combustion performance of bio-oils. Bioresour Technol 2014;152:267–74.
[45] Wilk M, Magdziarz A, Kalemba I. Characterisation of renewable fuels' torrefaction process with different instrumental techniques. Energy 2015;87:259–69.
[46] Chen WH, Kuo PC. A study on torrefaction of various biomass materials and its impact on lignocellulosic structure simulated by a thermogravimetry. Energy 2010;35:2580–6.
[47] Wilk M, Magdziarz A. Hydrothermal carbonization, torrefaction and slow pyrolysis of Miscanthus giganteus. Energy 2017:1–13.
[48] Jones JM, Nawaz M, Darvell LI, Ross AB, Pourkashanian M, Williams A. Towards biomass classification for energy applications. Science in Thermal and Chemical Biomass Conversion 2006;1:331–9.
[49] Brosse N, Dufour A, Meng X, Sun Q, Ragaukas A. Miscanthus: a fast growing crop for biofuels and chemicals production. Biofuels Bioprod Biorefin 2012;6:580–98.
[50] Jones MB, Walsh M. Miscanthus for energy and fibre. Earthscan; 2001.
[51] Basu P. Biomass gasification, pyrolysis and torrefaction-practical design and theory. Elsevier; 2013.
[52] Shan F, Lin Q, Zhou K, Wu Y, Fu W, Zhang P, et al. An experimental study of ignition and combustion of single biomass pellets in air and oxy-fuel. Fuel 2017;188:277–84.
[53] Basu P. Combustion and gasification in fluidized beds. CRC Press; 2006.